High-pressure sound velocity of perovskite-enstatite and the possible composition of the Earth's lower mantle

GONG Zizheng[1,2], XIE Hongsen[1], HUO Hui[2], JING Fuqian[2], GUO Jie[1] & XU Ji'an[2,3]

1. Material Laboratory of the Earth's Interior, Institute of Geochemistry, Chinese Academy of Sciences, Guiyang 550002, China;
2. Laboratory for Shock Waves and Detonation Physics Research, Southwest Institute of Fluid Physics, Chengdu 610003, China;
3. Institute of Geosciences, Academia Sinica, Taipei 11529, China
Correspondence should be addressed to Gong Zizheng (e-mail: gongzz@263.net)

Abstract The compressional sound velocity V_P for enstatite of polycrystalline specimens were measured at pressures from 40 to 140 GPa using the optical analytical techniques under shock loading. The dependence of V_P (in km/s) on Hugoniot pressure (P, in GPa) can be described by $\ln V_P = 3.079 - 0.691 \ln(P) + 0.094(\ln P)^2$. V_P satisfies Birch's law: $V_P = 4.068 + 1.677\rho$, where ρ is corresponding density, which indicated that enstatite is stable throughout the conditions of the lower mantle. The wave velocity P is 0.5% lower and the wave velocity S is 2% higher than that of PREM respectively. We concluded that the lower mantle is mainly composed of perovskite-$(Mg_{1-x}, Fe_x)SiO_3$ and only a small amount of $(Mg_{1-x}, Fe_x)O$ is allowed in it.

Keywords: enstatite, sound velocity, high-temperature and high-pressure, composition of the Earth's interior.

Generally, there are two constraints on the chemical composition of the Earth's interior. One is that the total composition of the Earth's interior must meet the bound of the cosmochemistry mode (element abundance of the solar system) and the data retrieved from the analysis of rocks on the Earth's surface. The other is that the substance composition of different Earth's interior layers must satisfy the geophysical mode based upon geophysical explorations of the Earth's interior (including density, gravity, and temperature distribution, elasticity property, electromagnetic property rheological property, etc). In other words, all the mineral assemblages that satisfy the two constraints should be possible candidates of the Earth's interior mineral composition. Obviously, this is an inversion problem with multiple solutions. Up to now, the understanding of mineral composition of the Earth's interior is mainly based on deep interior geophysical explorations and on the results of high-temperature and high-pressure experiments. Comparing the profiles of density and sound velocities (or bulk moduli) between seismological data and *in situ* measurement results of the candidate mineral assemblages under high-temperature and high-pressure, the main method is to constrain the possible substance composition of the Earth's interior[1−9]. Since the end of the 1970s, based upon lots of the studies on the equation of state and physical property under high pressure, it has become generally accepted that $(Mg_{1-x}, Fe_x)SiO_3$ with perovskite structure is the dominant phase of the lower mantle and the most abundant mineral in the Earth[10−14]. According to the density data obtained from the equation of state throughout the conditions of the lower mantle and the sound velocity (or bulk modulus) data at relatively low pressure, there are two kinds of opinions regarding the composition of the lower mantle under PREM constraints. One believes that the lower mantle is made of pyrolite, i.e. a mixture of about 80% (volume or weight) $(Mg_{1-x}, Fe_x)SiO_3$ and 20% $(Mg_{1-x}, Fe_x)O$, within which the ratio of Mg to Si is around 1.5−2, the upper and lower mantle is chemically homogeneous[4−6]. The other opinion believes that the lower mantle is made of chondrite, which means that it contains mainly $(Mg_{1-x}, Fe_x)SiO_3$ but only a small amount of $(Mg_{1-x}, Fe_x)O$ (the ratio of Mg to Si is 1). The lower mantle is primitive and undifferentiated, the upper and lower mantle is chemically inhomogeneous[7−9]. Hence, it is necessary to supplement the sound velocity experimental data of enstatite under relatively high pressure to decrease the multi-solvability of the problem about lower mantle composition and clarify the arguments above. However, no experimental sound speed (or thermal elasticity) of $(Mg_{1-x}, Fe_x)SiO_3$ are reported under pressure higher than 57 GPa[14].

On the other hand, several recent experiments conducted by Saxena et al.[15] and Meade et al.[16]

with a laser-heated diamond anvil cell showed that within the temperature range from 1 800 to 3 200 K, both (Mg, Fe)SiO_3 (pv) and pure $MgSiO_3$ (pv) dissociate to a mixture of SiO_2 (stishovite or an unquenchable polymorph) and (Mg, Fe)O (magnesiowustite) or MgO (periclase) under pressure of about 70 GPa. The decomposition is irreversible during the cooling and decreasing pressure process. Based on this, they suggested that the perovskite structure be unlikely stable in the lower mantle and the compositions of the mantle and the mineralogy model need to be reconsidered.

Sound velocity is relevant to the slope of material stress-strain curve; it is one of the most sensitive parameters reflecting the phase change under high temperature and high pressure. Thus, *in situ* measuring the sound velocity under high temperature and high pressure can show whether phase change happened. In this note, sound velocity for ($Mg_{0.92}$, $Fe_{0.08}$) SiO_3 with polycrystalline specimens were measured at pressure from 40 to 140 GPa using the optical analytical techniques under shock loading, in which the stability of enstatites (pv) and possible compositions of the lower mantle were discussed.

1 Experiments

(i) Expreimental samples. The enstatite samples studied in this experiment were made of the natural enstatite minerals, which were collected from Damaping, Hannuoba, Zhangjiakou, Hebei Province, China. The enstatite rock was ground into powder (<0.05 mm in diameter) using ball mill and was purified by the magnetic separation method using WCF2 multi-users magnetic analyzer. Then the mingling Fe powder was removed with magnetic and HCl liquid (there is no reaction between HCl liquid and enstatite). The powder then was hot pressed at 56 MPa and 1 400 K using graphite cylindrical mould in vacuum and pressed into disk-like samples with 15 mm in diameter and about 2, 3, 4 mm in thickness. The average density of initial samples is 3.07 g/cm^3. The chemical composition is SiO_2(54.72%), MgO(31.09%), FeO(5.00%), Al_2O_3 (4.02%), Fe_2O_3(2.44%), CaO(1.70%), and d values of X-Ray diffraction are 3.167(100), 2.876(64), 2.499(6) and 2.940(5) respectively.

(ii) Optical analytical technique[17]. The experiments were conducted with a 37-mm two-stage light-gas gun in Laboratory for Shock Wave and Detonation Physics Research by using metal flyer bearing projectiles to impact samples at speeds of up 6.8 km/s. The experimental assembly is shown in fig. 1.

Fig. 2 is the distance-time diagram in Lagrangian coordinates of wave propagation through the flyer and sample produced by the impact between the flyer and the base-plate. Three samples with the same diameter and different thicknesses (stepped-sample) are arranged in the same plane. The initially transparent bromoform (BF) is used as the optical analyzer medium and could emit thermal radiation from the shock front travelling in BF. Three thin optical fibers are used to monitor the light radiation from BF with intensities depending on shock pressure, which is employed to affirm the catch-up time of the release wave overtaking the shock front in BF and characterized by an abrupt decrease of radiation

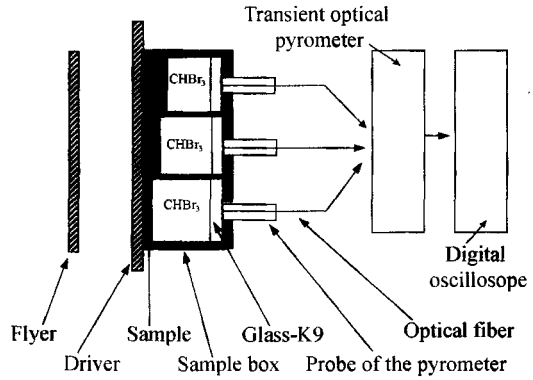

Fig. 1. Schematic diagram of experimental set-up and measuring system.

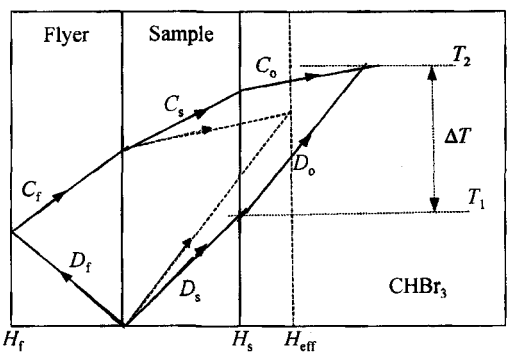

Fig. 2. Schematic diagram in Lagrangian coordinates of waves and their interaction in sample and flyer. D and C represent shock wave velocity and sound velocity respectively; f, s and o represent flyer, sample and $CHBr_3$ respectively.

intensity. Each fiber records the radiation history for every one step of the stepped-sample.

After impacting of flyer and sample, a right travelling shock wave D_s and a left travelling shock wave D_f were produced in sample and flyer respectively. T_1 denotes the arrival time of the shock wave D_f, which emerges from the sample/BF interface, T_2 denotes the catch-up time of the release sound wave, which is reflected from the free surface at the rear of the thin impacting flyer and travels back through the sample and BF, overtaking the shock front in BF detected optically. According to ref. [18], $\Delta T = T_2 - T_1$ and H_s the sample thickness, the intercept on the abscissa of the extrapolation of $\Delta T - H_s$ straight line defines a virtual sample thickness H_{eff}, at which the release wave would catch up the shock front in BF just at the sample/BF interface. The compressional sound velocity V_p is given by

$$V_p = [(\rho_0 / \rho) \times H_{eff}] / [(H_{eff} / D_s) - (H_f / D_f) - (H_f / V_f) \times (\rho_0 / \rho)], \quad (1)$$

where ρ is the sample density under shock loading and ρ_0 the initial density. H_{eff} is the effective thickness of the sample and was determined by our experiments. D_s and D_f are the shock velocities in sample and flyer respectively, H_f and V_f are the thickness and sound velocity of the flyer respectively. Experiment and the known Hugonit equation of state (EOS) can determine all of them. The results of enstatite Hugoniot EOS of Watts'[12]: $U_s = 4.83(\pm 0.42) + 1.22(\pm 0.10)\, u_p$, are utilized in data reduction.

2 Experimental results and discussion

Enstatite will be changed into the perovskite structure when the shock pressure is higher than 26 GPa[13, 14]. The range of the shock pressure of our experiments is 40—140 GPa (the temperature is about 1 000—5 000 K), so the sound velocity was measured for perovskite-enstatite. The dependence of the compressional sound velocity of enstatite (pv.) on Hugoniot pressure P fitted for five shots can be described by

$$\ln V_p = 3.079 - 0.691 \ln(P) + 0.094 (\ln P)^2, \quad (2)$$

where V_p is in km/s and P is in GPa. The sound velocity V_p determined by the experiment is 11.83 km/s at 66.34 GPa and 11.75 km/s at 84.03 GPa (figs. 3 and 4). It seems that there is a softening of the sound velocity between 66 and 85 GPa, and the pressure range of softening matches that of decomposition phase change[16]. It has been testified that for most metals, such as alkali metal compounds and quite a part of minerals and rocks, sound velocity (P wave, S wave or Bulk wave) would appear in a linear relationship with density when no phase transition happened (Birch's law)[18]. The relationship between the compressional sound velocity and the density for enstatite (pv) can be fitted with a single straight line (see fig. 3):

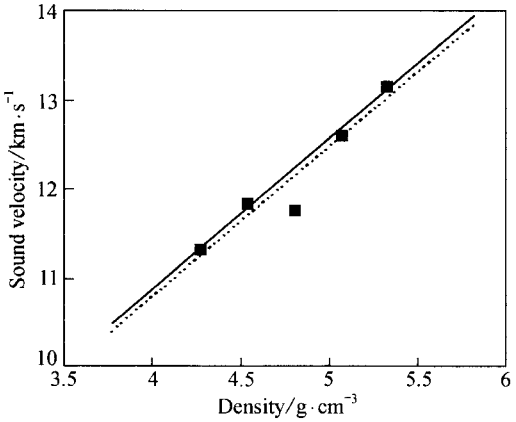

Fig. 3. The relationship between compressional sound velocity and density for enstatite (pv) along Hugoniot. ■ represent experimental data; solid line and dotted line represent experimental data fitted of all five points and 1, 2, 4, and 5 points respectively.

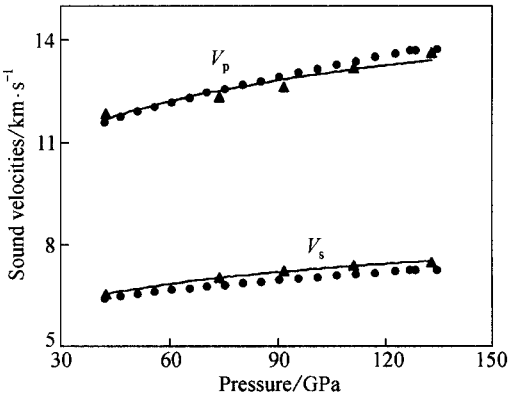

Fig. 4. Comparison of the compressional and shear sound velocities profiles with PREM lower mantle model. ▲ and solid curves represent experimental data and their fitted, respectively. ● represent PREM data.

$$V_p = 4.068 + 1.677\rho, \quad (3)$$

where ρ is corresponding density. This indicated that enstatite (pv) is stable in the temperature and pressure ranges of the lower mantle. Our conclusion was also supported by the newest experimental results from G. Serghiou et al.[19]. Sound velocities are typically determined to 3% precision using these techniques. Taking this into account, the lower deviation of sound velocity measured at 84.03 GPa is probably due to the experiment error.

After temperature correction, the comparison profiles of sound velocities between enstatite (pv) and PREM[20] are given in fig. 4. The shear wave velocity of enstatite (pv) is given by $V_s^2 = 3/4(V_p^2 - V_B^2)$, V_B is the bulk wave velocity and its value on Hugoniot is given by[21] $V_B = \left\{v_H^2(\gamma / v_H)(P_H / 2) - v_H^2(dP_H / dv_H)_p[1 - 1/2(\gamma / v_H)(v_{0H} - v_H)]\right\}^{1/2}$, where v_H and P_H are specific volume and pressure along Hugoniot respectively; γ is Grüneison parameter. Fig. 4 shows that in the pressure range of 40—140 GPa, the profiles of sound velocities of *P* wave and *S* wave for enstatite (pv) are parallel with that of PREM, and the two curves are very close. The *P* wave velocity is about 0.5% lower and the *S* wave velocity is about 2% higher than that of PREM respectively.

Considering the following two facts that both the isoentropic bulk modulus and shear modulus of $(Mg_{1-x}, Fe_x)O$ are only about half of that of $(Mg_{1-x}, Fe_x)SiO_3$, so the sound velocity for the mixture of $(Mg_{1-x}, Fe_x)SiO_3$ + $(Mg_{1-x}, Fe_x)O$ should be lower than that of $(Mg_{1-x}, Fe_x)SiO_3$, and it must be much lower with the increase of proportion for $(Mg_{1-x}, Fe_x)O$ in the mixture. Another fact that $(Mg_{1-x}, Fe_x)SiO_3$, in which x changes around 0.1, sound velocities (or bulk moduli) are very sensitive to the Si/(Mg + Fe) ratio but insensitive to the Fe/(Mg + Fe) ratio[14]. So we can take it for granted that under the constraints of wave profiles of PREM, the lower mantle is mainly composed of $(Mg_{1-x}, Fe_x)SiO_3$, which only permits a small amount of $(Mg_{1-x},Fe_x)O$ in it.

3 Conclusions

From the above we can draw following conclusions:

Enstatite (pv) is throughout stable under the lower mantle's temperature and pressure condition.

The profiles of the sound velocities of *P* wave and *S* wave for enstatite (pv) are parallel with that of PREM. The *P* wave velocity is about 0.5% lower and the *S* wave velocity is about 2% higher than that of PREM, respectively.

The lower mantle is mainly composed of $(Mg_{1-x}, Fe_x)SiO_3$, which only permits a small amount of $(Mg_{1-x},Fe_x)O$ in it. The lower mantle is chondritic or rich in enstatite.

Acknowledgements This work was supported by the National Natural Science Foundation of China (Grant No. 19672058) and the Science and Technology Foundation of the Chinese Academy of Engineering Physics (Grant No. 960103).

References

1. Xie Hongsen et al., Introduction to Material Science of the Earth's Interior (in Chinese), Beijing: Science Press, 1997, 75.
2. Zhu Rixiang, Li Chunjing, Pan Yongxin, Physics of the Earth's interior, Progress in Geophysics, 1997, 12: 65.
3. Gong Zizheng, Bi Yan, Application of shock wave physics to the earth and planetary science (in Chinese), Progress in Geosciences, 1997, 12: 399.
4. Rinrwood, A. E., Composition and Petrology of the Earth's Mantle, New York: Mcgraw-Hill, 1975, 618.
5. Anderson, O. L., Finding the isentropic density of perovskite: Implications for iron concentration in the lower mantle, Geophys. Res. Lett., 1997, 24: 213.
6. Stacey, F. D., Thermoelasticity of (Mg,Fe)SiO_3 perovskite and a comparison with the lower mantle, Phys. Earth Planet. Inter., 1996, 98: 66.
7. Anderson, D. L., Composition in the Mantle and Core, Ann. Rev. Earth Planet. Sci., 1977, 5: 179.
8. Stixrude, L., Hemley, R. J., Fei, Y., Mao, H. K., Thermoelasticity of silicate perovskite and magnesiowustite and stratification of the Earth's mantle, Science, 1992, 257: 1099.
9. Zhao Yusheng, Anderson, D. L., Mineral physics constraints on the chemical composition of the Earth's lower mantle, Phys. Earth Planet. Inter., 1994, 85: 273.
10. Liu, L. G., Orthorhomic perovskite phases observed in olivine, pyroxene and garnet at high pressures and temperatures, Phys. Earth Planet. Inter., 1976, 11: 289.
11. Knittle, E., Jeanloz, R., Synthesis and equation of state of (Mg, Fe) SiO_3 perovskite to over 100 GPa, Science, 1987, 235: 668.

12. Watt, J. P., Ahrens, T. J., Shock wave equation of state of enstatite, J. Geophys. Res., 1986, B91: 7495.
13. Wang Yanbin, Weidner, D. J., Liebermann, R. C., Zhao Yusheng, P-V-T equation of state of (Mg, Fe)SiO_3 perovskite: constraints on composition of the lower mantle, Phys. Earth Planet. Inter., 1994, 83: 13.
14. Guillaume, Andrault, F. D. et al., P-V-T equation of state of $MgSiO_3$ perovskite, Phys. Earth Planet. Inter., 1998, 105: 21.
15. Mead, C., Mao Ho Kwang, Hu Jingzhu, High-Temperature Phase transition and dissociation of (Mg, Fe)SiO_3 perovskite at Lower Mantle pressure, Science, 1995, 268: 1743.
16. Saxena, S. K., Dubrovinsky, L. S., Lazor, P. et al., Stability of perovkite $MgSiO_3$ in the Earth's Mantle, Science, 1996, 274: 1357.
17. McQueen, R. G., Hopson, J. W., Fritz, J. N., Optical technique for determining rarefaction wave velocities at very high Pressure, Rev. Sci. Instru., 1982, 53: 245.
18. Campbell, A. J., Heinz, D. L., A high-pressure test of Birch's law, Science, 1992, 257: 66.
19. Serghiou, G., Zerr, A., Boehler, R., (Mg, Fe)SiO_3-perovskite stability under lower mantle conditions, Science, 1998, 280: 2093.
20. Dziewonski, A. M. and Anderson, O. L., Preliminary reference earth model, Phys. Earth Planet. Inter., 1981, 25: 297.
21. Jing Fuqian et al., Introduction to Experimental Equation of State (in Chinese), Beijing: Science Press, 1986, 323.

(Received April 16, 1999; accepted November 30, 1999)